ISSN 1075-7015, Geology of Ore Deposits, 2015, Vol. 57, No. 7, pp. 570–578. © Pleiades Publishing, Ltd., 2015.
Original Russian Text © M.V. Charykova, E.L. Fokina, V.G. Krivovichev, O.S. Yakovenko, E.V. Klimova, V.V. Semenova, 2014, published in Zapiski Rossiiskogo Mineralogicheskogo Obshchestva, 2014, No. 3, pp. 72–84.

Thermodynamics of Arsenates, Selenites, and Sulfates in the Oxidation Zone of Sulfide Ores. X. Thermal Stability and Dehydration Features of Synthetic Analogs of the Cobaltomenite–Ahlfeldite Solid Solution Series

M. V. Charykova, E. L. Fokina, V. G. Krivovichev, O. S. Yakovenko, E. V. Klimova, and V. V. Semenova

St. Petersburg State University, Universitetskaya nab. 7/9, St. Petersburg, 199034 Russia

Received February 12, 2013

Abstract—The aim of this study is the experimental investigation of the synthetic analogs of cobaltomenite, $CoSeO_3 \cdot 2H_2O$, ahlfeldite, $NiSeO_3 \cdot 2H_2O$, members of the cobaltomenite–ahlfeldite solid solution series $(Ni_xCo_{1-x})SeO_3 \cdot 2H_2O$, and singularities of their dehydration and dissociation. The intermediate members of the cobaltomenite ($CoSeO_3 \cdot 2H_2O$)–ahlfeldite ($NiSeO_3 \cdot 2H_2O$) series have been synthesized and studied with a combination of X-ray diffraction, scanning electron microscopy, and the simultaneous application of thermogravimetry (TG) and differential scanning calorimetry (DSC) within the temperature range from 25 to 640°C. The complete solid solution series corresponds to the monoclinic space group $P2_1/n$. Unit-cell dimensions decrease in all crystallographic directions as the amount of Ni increases. The angle β increases from 98.82(1) (cobaltomenite) to 99.05(1)° (ahlfeldite). It has been established that $CoSeO_3 \cdot 2H_2O$ and $NiSeO_3 \cdot 2H_2O$ dehydrate at 120–340°C through two stages apparently corresponding, to the formation of intermediate hydrated species $CoSeO_3 \cdot H_2O$ and $NiSeO_3 \cdot 1/3H_2O$. The reaction enthalpies for each dehydration stage of $CoSeO_3 \cdot 2H_2O$ and $NiSeO_3 \cdot 2H_2O$ have been determined. Changes of the unit-cell dimensions and dehydration temperatures are rationalized in terms of the Co and Ni site occupancy in the structure of the cobaltomenite–ahlfeldite solid-solution series members.

DOI: 10.1134/S107570151507003X

INTRODUCTION

This study continues a series of investigations of thermal stability and dehydration features of hydrous selenites (Fokina et al., 2014; Charykova et al., 2014), which are formed under seasonal fluctuation of temperature in a near-surface setting involving aqueous solutions and ambient pressure and are found, as rule, in the oxidation zone of sulfide- and selenide-bearing ores. Cu, Co, Ni, and Fe are species-defining cations of these minerals (ahlfeldite, chalcomenite, cobaltomenite, mandarinoite).

The synthetic analogs of cobaltomenite, $CoSeO_3 \cdot 2H_2O$ and ahlfeldite, $NiSeO_3 \cdot 2H_2O$, and $(Ni_xCo_{1-x})SeO_3 \cdot 2H_3O$ solid solution members were studied, because natural ahlfeldite and cobaltomenite form complete solid-solution series (Sturman and Mandarino, 1974; Larrañaga et al., 2005). Ahlfeldite and cobaltomenite are rather rare minerals precipitated only in the oxidation zone of sulfide and selenide ores.

Cobaltomenite was discovered from the Cerro de Cacheuta deposit in Argentina in association with chalcomenite, molybdomenite, olsacherite, cerussite, and azurite (Bertrand, 1882). Ahlfeldite was described for the first time from the Pacajake deposit, Bolivia in oxidized ores in association with chalcomenite, cobaltomenite, molybdomenite, native selenium, olsacherite, and mandarinoite (Herzenberg and Ahlfeld, 1935; Aristarain, Hurlbut, 1969).

The thermal behavior of synthetic $CoSeO_3 \cdot 2H_2O$ and $NiSeO_3 \cdot 2H_2O$ has previously been studied by Makatun et al. (1973), Vlaev et al. (2005, 2006), and Larrañaga et al. (2005). However, despite sufficiently detailed study, some aspects remain not quite clear. First, this is related to the dehydration features of $CoSeO_3 \cdot 2H_2O$ and $NiSeO_3 \cdot 2H_2O$ and probable formation of intermediate hydrated species as a result of thermal dehydration. These species, which are synthetic crystal hydrates of Ni and Co selenites containing 1 and 1/3 water molecules, are reported in the literature (e.g., Makatun et al., 1974, 1975); their structural parameters are reported by Wildner (1991) and Engelen et al. (1996), respectively. The intermediate phases as dehydration products of $CoSeO_3 \cdot 2H_2O$ and $NiSeO_3 \cdot 2H_2O$ during thermal analysis are not identified in any aforementioned articles (Makatun et al., 1973, 1974; Vlaev et al., 2005, 2006; Larrañaga et al., 2005).

Corresponding author: Charykova M.V. E-mail: m.charykova@spbu.ru

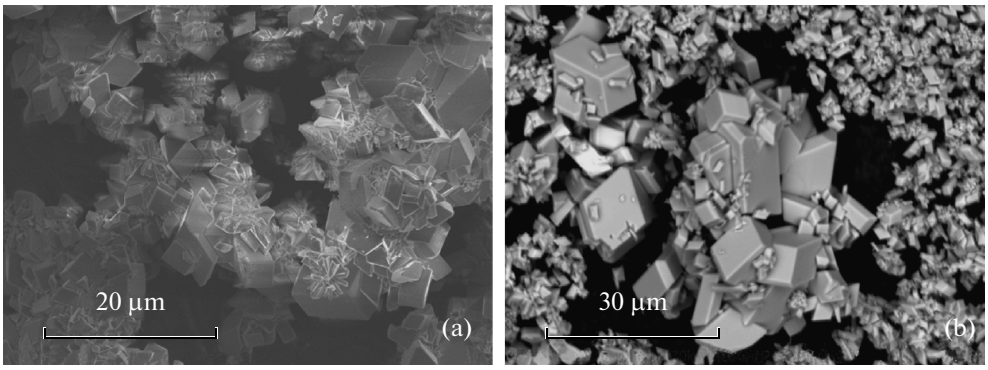

Fig. 1. Morphology of synthesized crystals of (a) cobaltomenite and (b) ahlfeldite.

α- and β-$CoSeO_3 \cdot 1/3H_2O$ and α- and β-$NiSeO_3 \cdot 1/3H_2O$ (along with two crystal hydrates) were obtained by Vlaev et al. (2005, 2006) as a part of the experimental study of solubility in the $CoSeO_3$–SeO_2–H_2O and $NiSeO_3$–SeO_2–H_2O systems within the temperature range from 25 to 300°C. The transition of $NiSeO_3 \cdot 2H_2O$ and $CoSeO_3 \cdot 2H_2O$ to monohydrate crystal hydrates was not established.

The stages of dehydration of $CuSeO_3 \cdot 2H_2O$ (synthetic analog of chalcomenite) and $ZnSeO_3 \cdot 2H_2O$ were previously established by Fokina et al. (2014) and Charykova et al. (2014). In this study, the dehydration of $CoSeO_3 \cdot 2H_2O$ and $NiSeO_3 \cdot 2H_2O$ is discussed.

SYNTHESIS OF AHLFELDITE AND COBALTOMENITE ANALOGS

The slightly modified method elaborated by Vlaev et al. (2005, 2006) has been applied to the synthesis of Co and Ni selenites from the solutions of Co and Ni nitrates and Na selenite acidified by nitric acid solution. The 0.2N solution of $NaSeO_3$ (pH 6.0–6.2) was added slowly drop-by-drop to a 0.2N solution of Ni or Co salt (pH 5.2–5.3) heated to 50°C. After heating for 2–3 h and weak stirring, the solution with precipitate matured for 20 days at room temperature; then the precipitate was decanted, washed with distilled water, and dried at room temperature.

The substances obtained are pink-purple (Co selenite) or green (Ni selenite) fine columnar crystals (Fig. 1). The synthetic solid phases were determined with the X-ray powder diffraction (Rigaku Miniflex II powder diffractometer) and IR spectroscopy (BRUKER VERTEX 80 IR-Fourier spectrometer). The chemical composition of solid phases was measured on a Hitachi S-3400N SEM and ICP-MS (after acid decomposition). The concentration of Co, Ni, and Se in the solutions was determined with ICP-MS on an ELAN-DRC-e PERKIN ELMER instrument.

COMPLEX THERMAL ANALYSIS

The behavior of $CoSeO_3 \cdot 2H_2O$ and $NiSeO_3 \cdot 2H_2O$ was investigated on a STA 449 F3 Jupiter synchronous thermal analyzer allowing simultaneous determination of weight loss (thermogravimetric analysis) and thermal effects (differential scanning calorimetry) with linear temperature programming. Dehydration of the sample was studied within the range from 25 to 640°C; a corundum crucible was used. The weight of the samples was 13.611 mg ($CoSeO_3 \cdot 2H_2O$) and 17.979 mg ($NiSeO_3 \cdot 2H_2O$), with a heating rate of 2°/min. The results were processed with the program NETZSCH Proteus Thermal analysis v. 5.2.1. The Peak Separation v. 2010.09 was used for additional detailed processing of the DSC curve and separation of the effects; the DSC curve was fitted with Gaussian function.

The results of thermal analysis of $CoSeO_3 \cdot 2H_2O$ (TG, DTG, and DSC curves) are shown in Figs. 2 and 3. Figure 2, pertaining to the temperature range of sample dehydrationm exhibits two endothermic effects accompanied by weight loss on the DSC curve. The first effect appears within the temperature range 120–195°C (T_{max} = 165.8°C), the second effect appears within the range 235–275°C (T_{max} = 255.7°C). The total weight loss of both effects is 16.21 wt %. The value obtained is consistent with the calculated weight change (16.24%) with removal of two water molecules from cobaltomenite according to the reaction:

$$CoSeO_3 \cdot 2H_2O \rightarrow CoSeO_3 + 2H_2O.$$

In the sample studied here, the weight loss at each stage is 8.03 and 8.18%. Thus, cobaltomenite is suggested to be dehydrated in two stages with loss of one water molecule at each stage; i.e., monohydrate $CoSeO_3 \cdot H_2O$ is an intermediate phase. We have calculated dehydration enthalpies for each stage: ΔH_1 = 44.1 kJ/mol and ΔH_2 = 30.4 kJ/mol; total is 74.5 kJ/mol. Previously, Fokina et al. (2014) and Charykova et al. (2014) calculated dehydration

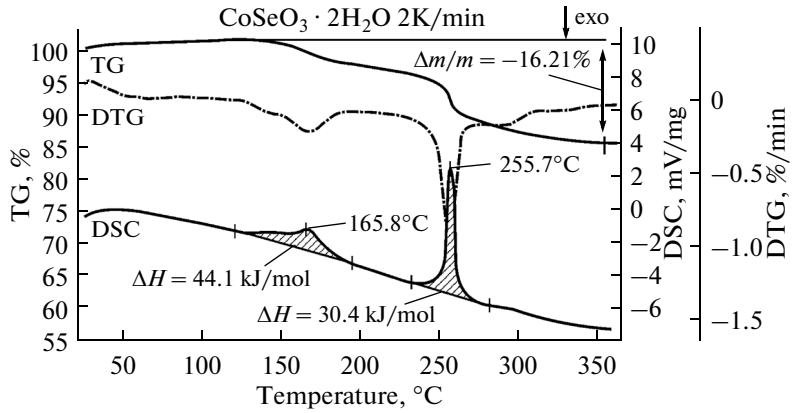

Fig. 2. Results of complex thermal analysis (DSC, TG, DTG curves) of $CoSeO_3 \cdot 2H_2O$ within temperature range 25–380°C

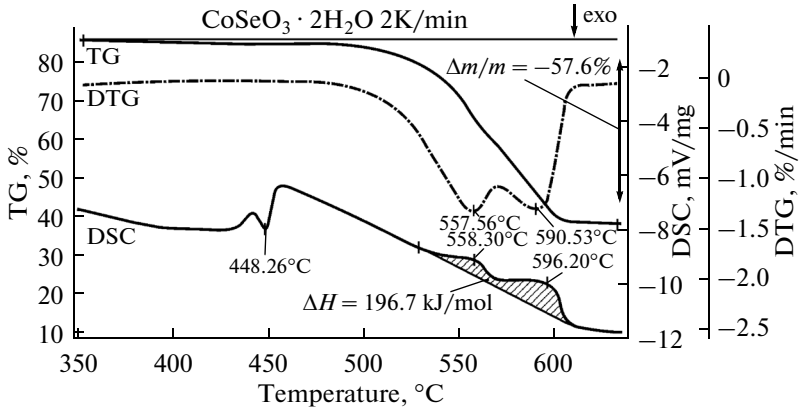

Fig. 3. Results of complex thermal analysis (DSC, TG, DTG curves) of $CoSeO_3 \cdot 2H_2O$ within the temperature range 350–650°C

enthalpies for $CuSeO_3 \cdot 2H_2O$ 67.4 kJ/mol and $ZnSeO_3 \cdot 2H_2O$ 98.33 kJ/mol, respectively.

The further heating of the sample (Fig. 3) results in an exothermal effect at 448.3°C apparently corresponding to the crystallization of amorphous anhydrous cobalt selenite. Then, $CoSeO_3$ decomposes within the temperature range 533–608°C with peaks at 558.3 and 596.2°C. Total weight loss (57.6%) is consistent with the calculated value (59.7%) with the decomposition of anhydrous cobalt selenite according to the reaction:

$$CoSeO_3 = CoO + SeO_2.$$

Calculated decomposition enthalpy is 196.7 kJ/mol.

The results of thermal analysis of $NiSeO_3 \cdot 2H_2O$ are shown in Figs. 4 and 5. Two endothermic effects within the temperature range 140–340°C are observed on the DSC curve (Fig. 4). The first effect is related to the maximum at 210.8°C; the second effect is very fuzzy on the DSC curve, but is clear on the DTG curve with a peak at 323.0°C. The both effects are accompanied with a total weight loss of 16.29%, which is consistent with the calculated value of weight change (16.25%) for the removal of two water molecules from ahlfeldite according to the reaction:

$$NiSeO_3 \cdot 2H_2O \rightarrow NiSeO_3 + 2H_2O.$$

The correct determination of weight loss for each effect on the TG curve is impossible; however, it could be done in regard to the relationship of peak areas on the DTG curve: weight loss ratio is 5 : 1; i.e., the loss of 1/3 water molecule corresponds to the second effect. Thus, ahlfeldite is suggested to dehydrate during two stages; however, in this case, the intermediate phase is $NiSeO_3 \cdot (1/3)H_2O$ in contrast to monohydrate in the case of cobaltomenite.

The calculated total enthalpy of dehydration is 98.7 kJ/mol. Vlaev et al. (2006) published a value of 89.0 kJ/mol.

For further heating within the temperature range from 510 to 640°C (Fig. 5), the sample breaks down during two stages at 564.0 and 624.1°C. The effects are well seen in the DSC and DTG curves; the areas of corresponding peaks on the DTG curve are not equal.

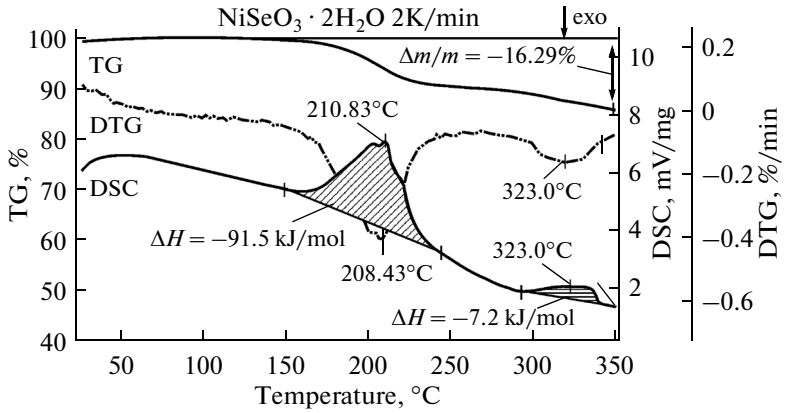

Fig. 4. Results of complex thermal analysis (DSC, TG, DTG curves) of $NiSeO_3 \cdot 2H_2O$ within temperature range 25–420°C.

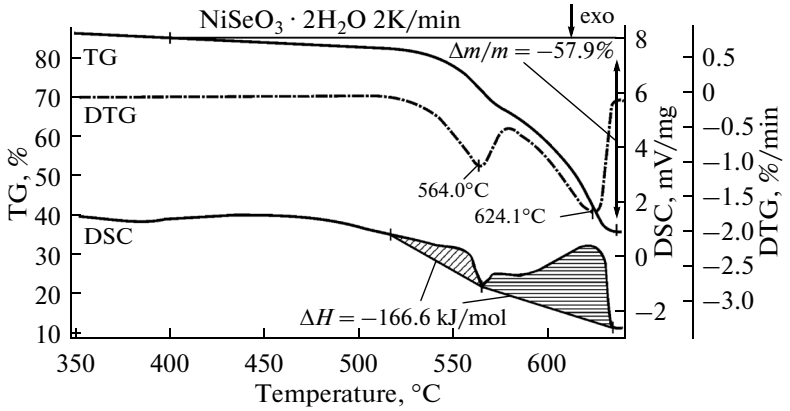

Fig. 5. Results of complex thermal analysis (DSC, TG, DTG curves) of $NiSeO_3 \cdot 2H_2O$ within temperature range 400–640°C.

Total weight loss of 57.9% is consistent with the calculated value (59.8%) related to decomposition of anhydrous Ni selenite according to the reaction:

$$NiSeO_3 = NiO + SeO_2.$$

The calculated total enthalpy of decomposition is 166.6 kJ/mol. Vlaev et al. (2006) obtained 181.5 kJ/mol.

Our results of thermal analysis of cobaltomenite and ahlfeldite as compared with data from the literature are given in Table 1.

SYNTHESIS AND PROPERTIES OF COBALTOMENITE–AHLFELDITE SOLID SOLUTIONS

The thermal analysis of synthetic analogs of cobaltomenite and ahlfeldite has shown a significant difference in their behavior under the effect of heating, in particular as concerns the formation of distinct intermediate phases in the course of dehydration. Therefore, the study of the intermediate members of the $(Ni_xCo_{1-x})SeO_3 \cdot 2H_2O$ solid solution series is of spe-

Table 1. Results of thermal analysis of $CoSeO_3 \cdot 2H_2O$ and $NiSeO_3 \cdot 2H_2O$ as compared with published data

Process	Temperature range, °C		
	Larrañaga et al., 2005	Vlaev et al., 2005, 2006	Our data
Dehydration			
CoSeO · 2HO		260 (T_{max})	120–275
$NiSeO_3 \cdot 2H_2O$	<350	290 (T_{max})	140–340
Decomposition			
$CoSeO_3 \cdot 2H_2O$	450–525	487–680	533–608
$NiSeO_3 \cdot 2H_2O$		600–700	510–640

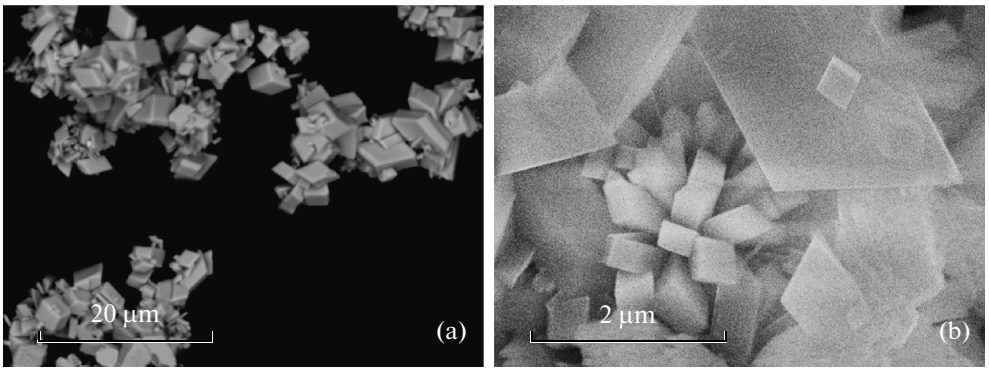

Fig. 6. Morphology of solid solution crystals: (a) $(Ni_{0.55}Co_{0.45})SeO_3 \cdot 2H_2O$ and (b) $(Ni_{0.74}Co_{0.26})SeO_3 \cdot 2H_2O$.

cial interest. Solid solutions of Co and Ni selenites were synthesized according to the procedure applied for synthesis of the end members. Synthesis was carried out from the solutions prepared by mixing of 0.2N Co and Ni nitrate solutions and Na selenite acidified by nitric acid. The synthesized phases were identified with the aforementioned techniques.

The synthesized phases $(Ni_xCo_{1-x})SeO_3 \cdot 2H_2O$ (x ranges from 0.05 to 0.83) are bright to pale pink fine crystals (Fig. 6). It is noteworthy that even crystals with the highest Ni content synthesized from the solutions with a Ni : Co value of 93 : 7 are pink–beige rather than green.

The relationships of Ni and Co in initial solutions, from which solid phases of variable composition were synthesized, are shown in Table 2. The mole fraction of $Ni(NO_3)_2$ in the mixed solution of Ni and Co nitrates X^L_{Ni} is $m(Ni(NO_3)_2)/[m(Ni(NO_3)_2) + m(Co(NO_3)_2)]$, where m is molar concentration and the mole fraction of $NiSeO_3 \cdot 2H_2O$ in solid solutions is $(Ni_xCo_{1-x})SeO_3 \cdot 2H_2O$.

The compositions of aqueous solutions formed during the 30-day interaction of the synthesized solid phases with water and proportion of Ni selenite in total molar concentration of selenites in saturated solutions $X^L_{Ni} = m(NiSeO_3)/[m(NiSeO_3) + m(CoSeO_3)]$ are given in the three last columns of Table 2. These data were obtained as a result of the experimental determination of solubility in the $CoSeO_3$–$NiSeO_3$–H_2O system with isothermal saturation in ampoules at 25°C for solid solutions $(Ni_xCo_{1-x})SeO_3 \cdot 2H_2O$ with $x = 0$, 0.05, 0.08, 0.11, 0.19, 0.35, 0.47, 0.60, 0.65, 0.83, and 1. The experimental procedure was described by Charykova et al. (2012), when it was applied to the study of solubility in the binary $CoSeO_3$–H_2O and $NiSeO_3$–H_2O systems. A small amount of solid phase was covered with distillated water and placed into thermostat shaker for 30 days; then the precipitate

Table 2. Compositions of liquid and solid solutions during synthesis of cobaltomenite–ahlfeldite solid solution analogs and for experimental determination of their solubility in water at 25°C

Sample	Fraction of Ni in Co + Ni sum in initial nitrate solution	Fraction of Ni (x) in solid solution $(Ni_xCo_{1-x})SeO_3 \cdot 2H_2O$	Content in saturated solution, mmol/L		Fraction of Ni in Co + Ni sum in saturated solution
			$CoSeO_3$	$NiSeO_3$	
1	0	0	0.058	0	0
2	0.10	0.05	0.062	0.004	0.058
3	0.21	0.08	0.056	0.005	0.082
4	0.29	0.11	0.063	0.008	0.11
5	0.46	0.19	0.067	0.013	0.16
6	0.55	0.35	0.063	0.033	0.34
7	0.65	0.47	0.060	0.047	0.44
8	0.74	0.60	0.028	0.025	0.47
9	0.85	0.65	0.021	0.024	0.53
10	0.93	0.83	0.010	0.027	0.73
11	1	1	0	0.029	1

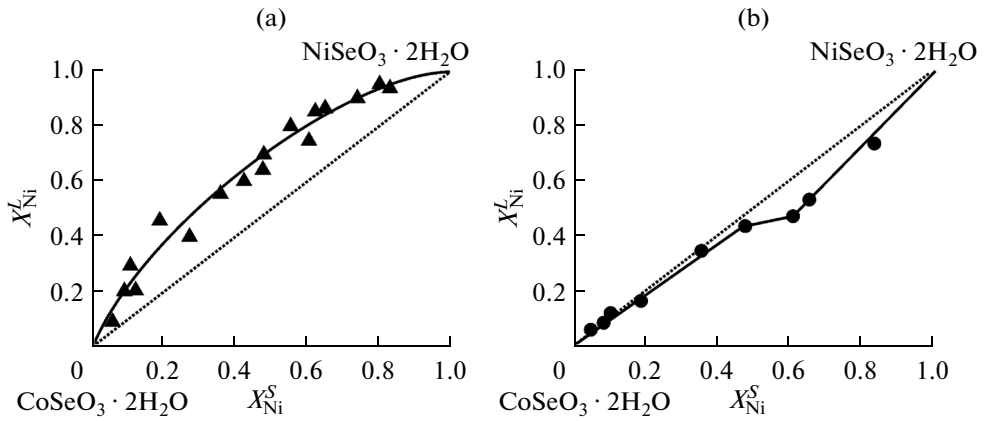

Fig. 7. (a) Compositions of liquid and solid phases during synthesis of $(Ni_xCo_{1-x})SeO_3 \cdot 2H_2O$ solid solutions, (b) partition of Ni and Co selenites between liquid and solid solutions after 30-day saturation at 25°C. X^S_{Ni} is Ni fraction in solid phase; X^L_{Ni} is Ni fraction in total molar concentration in solution. Dashed line corresponds to equal fractions of Ni in solid and liquid phases. Filled triangles denote composition of solutions during synthesis; circles denote composition of solutions after 30-day interaction of solid selenites with water.

separated by centrifugation and filtration was examined with X-ray powder diffraction, and contents of Co, Ni, and Se were determined in a saturated solution. It should be noted that we do not name these concentrations as equilibria; as previously shown, the obtained concentrations of saturated solutions actually are certain stationary contents of constituents resulted from interaction of solid selenites with water, which do not correspond to true thermodynamic equilibrium.

The same data are shown for clarity in Fig. 7: the Ni fraction in solid phase is denoted as X^S_{Ni} (on *x*-axis) and its fraction in total molar concentration of salts dissolved in liquid phase is X^L_{Ni} (on the *y*-axis). The compositions that correspond to the partition of components between solid phases and the solutions from which synthesis has been performed are marked by triangles (Fig. 7a) and partition between solid and liquid solutions after isothermal saturation is marked by circles (Fig. 7b). Dashed line in this figure corresponds to equal fractions of Ni in liquid and solid phase ($X^S_{Ni} = X^L_{Ni}$). The data in Table 2 and Fig. 7a show that the solid phase is substantially depleted in Ni as compared with the solution from which it was synthesized. After the interaction of the $(Ni_xCo_{1-x})SeO_3 \cdot 2H_2O$ compounds with water over 30 days, the proportion of Ni and Co in the solution remains almost the same as in the solid phase, when the Ni mole fraction is lower than ~ 0.05. Above $X \sim 0.6$, an appreciably less amount of Ni than that of Co passes into solution over the same time and under the same saturation conditions.

Martens et al. (2005), who studied solid solutions of Co and Ni arsenates (synthetic analogs of the erythrine–annabergite solid solution), established a relationship similar to that shown in Fig. 7a. As possible explanation of a higher Co content in solid solution as compared with that in the initial liquid solution, from which synthesis has been performed, the authors suggest a difference in the solubility of $Co_3(AsO_4)_2 \cdot 8H_2O$ and $Ni_3(AsO_4)_2 \cdot 8H_2O$ or distinct positions of Co and Ni ions in the structure of mixed $(Co,Ni)_3(AsO_4)_2 \cdot 8H_2O$ arsenates: Co ions preferably occupy site M(2), whereas Ni ions occupy site M(1) with proportion of these sites at 2 : 1. The preferred second explanation is supported by the relationships of the unit-cell dimensions and compositions of solid solutions, as well as IR and Raman spectroscopic data (Martens et al., 2005). As concerns difference in solubility product of erythrine and annabergite by three orders, Charykova et al. (2013) has noted that the literature data on the solubility of the minerals mentioned by Martens et al. (2005) are suspicious and require refinement.

Our experimental data on the solubility are shown in Fig. 8 as isotherm in coordinates of mole fractions. In contrast to Fig. 7b, the mole fractions of Ni, Co, and water in liquid and solid phases are related to the $CoSeO_3$–$NiSeO_3$–H_2O system, i.e., $X_{Ni} = n(NiSeO_3)/[n(NiSeO_3) + n(CoSeO_3) + n(H_2O)]$, $X_{Co} = n(CoSeO_3)/[n(NiSeO_3) + n(CoSeO_3) + n(H_2O)]$, and $X_{H_2O} = n(H_2O)/[n(NiSeO_3) + n(CoSeO_3) + n(H_2O)]$, where *n* is the number of moles of components. Inasmuch as concentrations in liquid phase are extremely low, they are shown in the figure on an augmented scale. Despite conditional character of the data (see above), we can state with confidence that the isotherm contains two branches of solid phase crystallization. Charykova et al. (2007) calculated the solubility isotherm in the $CoSeO_3$–$NiSeO_3$–H_2O system at 25°C using data from the literature on lnSP of $CoSeO_3 \cdot 2H_2O$ and $NiSeO_3 \cdot 2H_2O$ under the

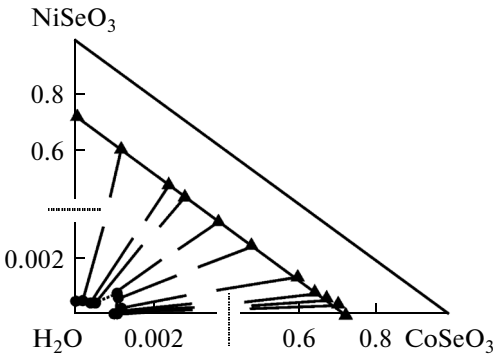

Fig. 8. Solubility plot of $CoSeO_3$–$NiSeO_3$–H_2O system at 25°C in coordinates of mole fractions. Compositions of solutions and solid phases are solid circles and triangles, respectively.

assumption of an ideal continuous series of solid solutions. The isotherm calculated in this way is one branch of crystallization of solid phases and does not contain nonvariant points. The experimental data do not support this assumption. To all appearances, there is a certain change in structure of the $(Ni_xCo_{1-x})SeO_3 \cdot 2H_2O$ solid solutions, and the solubility diagram consists of two branches corresponding to the crystallization of solid solutions based on $CoSeO_3 \cdot 2H_2O$ (nearly vertical line in Fig. 8, outgoing from the composition of saturated solution in the $CoSeO_3$–H_2O system) and $NiSeO_3 \cdot 2H_2O$ (line outgoing from the composition of saturated solution in the $NiSeO_3$–H_2O system). Unfortunately, we failed to establish the intersection of these two branches corresponding to eutonic equilibrium of solution with two solid phases in experiments. Therefore, this segment of the solubility isotherm is shown in Fig. 8 as conjectural by a dashed line.

The relationships between unit-cell dimensions and composition of solid solutions are shown in Fig. 9. As follows from this figure, the unit-cell dimension decreases from cobaltomenite to ahlfeldite in accordance with smaller ion radius of Ni as compared with that of Co (0.69 and 0.75 Å, respectively). A decrease in all three parameters a, b, and c becomes more sharp, when the Ni mole fraction is reaching 0.7–0.8. Additional spectroscopic and crystallographic study is required for interpreting these relationships (change of slope in all three plots). It is probably caused by the ordering of Ni and Co in the crystal structures of these compounds as has been established by Martens et al. (2005) in the erythrine–annabergite solid solution series.

Complex thermal analysis was performed for the $Ni_xCo_{1-x})SeO_3 \cdot 2H_2O$ (x = 0.12, 0.27, 0.42, 0.55, 0.62, 0.74, 0.80) solid solutions. The experimental conditions are similar to those reported for $CoSeO_3 \cdot 2H_2O$ and $NiSeO_3 \cdot 2H_2O$. The weight of samples was from 11.017 to 34.563 mg. The generalized dehydration and decomposition temperatures are given in Table 3 and Fig. 10. According to these data, all members of the solid solution series were dehydrated during two stages with increasing dehydration temperature at the first and the second stages as Ni concentration increases; in addition, the character of dehydration changes. In the samples with Ni fraction $X < 0.42$, water is lost as in the pure cobaltomenite, i.e., via the formation of monohydrate crystalline hydrate $(Ni_xCo_{1-x})SeO_3 \cdot H_2O$, whereas since the sample with $X = 0.42$, crystalline hydrate $(Ni_xCo_{1-x}) \cdot SeO_3 \cdot 1/3H_2O$ has become an intermediate phase. For samples with Ni concentrations ranging from 0.42 to 0.80, an additional endothermic peak appears in the thermal curves in the region corresponding to dissociation. It can be suggested that this peak corresponds to the transition of α-$(Ni_xCo_{1-x}) \cdot SeO_3 \cdot 1/3H_2O$ to the β modification.

Table 3. Results of thermal analysis of samples of the $(Ni_xCo_{1-x})SeO_3 \cdot 2H_2O$ isomorphic series

Ni fraction (x) in the $(Ni_xCo_{1-x})SeO_3 \cdot 2H_2O$ solid solution	Dehydration temperature, °C			Decomposition temperature, °C	
	T_1	T_2	T_3	T_1	T_2
0	165.8	255.7		558.3	596.2
0.12	176.5	260.8		568	628.2
0.27	175.2	261.5			614.3
0.42	189	266.9	281.7		627.7
0.47	197.5	270	284.5		620
0.55	193.4	278	294.5		613.9
0.62	198.2	284	299.4		612.7
0.74	185.3	285.1	290		611.3
0.8	198.7	296.8	–		615.5
1	210.8	323	–	564	624.1

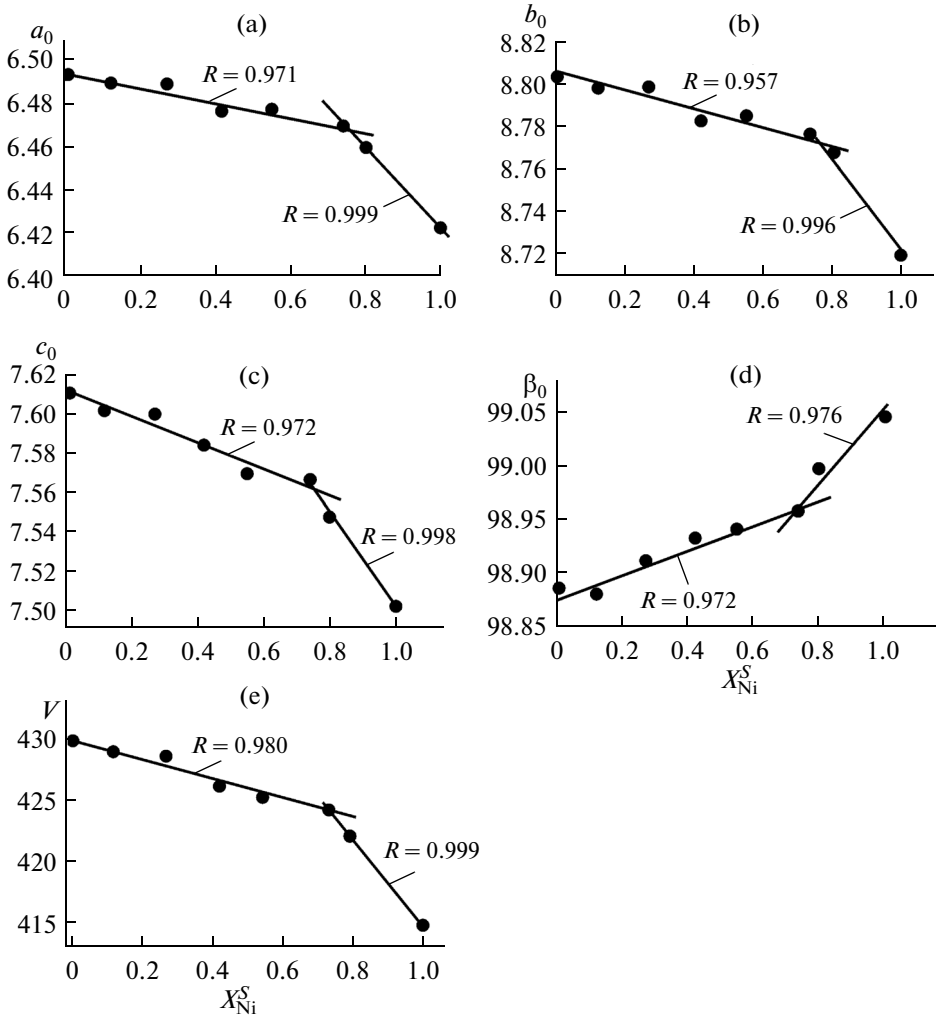

Fig. 9. Unit-cell parameter versus Ni mole fraction for the $(Ni_xCo_{1-x})SeO_3 \cdot 2H_2O$. *R* denotes correlation coefficient.

Thus, the results obtained assume three probable variants of thermal dissociation in the cobaltomenite–ahlfeldite solid solution:

(I) $(Ni_xCo_{1-x})SeO_3 \cdot 2H_2O \rightarrow (Ni_xCo_{1-x})SeO_3 \cdot H_2O \rightarrow (Ni_xCo_{1-x})SeO_3$ for cobaltomenite and solid solutions with the Ni fraction $X < \sim 4$;

(II) $(Ni_xCo_{1-x})SeO_3 \cdot 2H_2O \rightarrow (Ni_xCo_{1-x})SeO_3 \cdot 1/3H_2O \rightarrow (Ni_xCo_{1-x})SeO_3$ for ahlfeldite and solid solutions with the Ni fraction $X > \sim 0.8$;

(III) $(Ni_xCo_{1-x})SeO_3 \cdot 2H_2O \rightarrow \alpha\text{-}(Ni_xCo_{1-x})SeO_3 \cdot 1/3H_2O \rightarrow \beta\text{-}(Ni_xCo_{1-x})SeO_3 \cdot 1/3H_2O \rightarrow (Ni_xCo_{1-x})SeO_3$ for solid solutions with the Ni fraction $\sim 0.4 < X < \sim 8$.

The data obtained suggest the probable formation of not only members of the cobaltomenite–ahlfeldite solid solution in the oxidation zone of selenium-bearing sulfide ores, but other Ni and Co selenites with variable content of crystallization water.

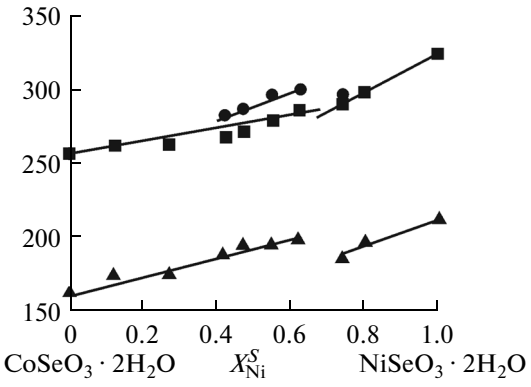

Fig. 10. Temperature of dehydration and decomposition of $(Ni_xCo_{1-x})SeO_3 \cdot 2H_2O$ solid solution. Solid triangles, squares, and circles denote the first, second, and third stages of dehydration, respectively.

ACKNOWLEDGMENTS

This study was supported by St. Petersburg State University (grant no. 3.38.286.2015) and performed using the equipment of the Resource Centers for X-ray diffraction methods and Geomodel at this university.

REFERENCES

Aristarain, L.F. and Hurlbut C.S., Jr., Ahlfeldite from Pacajake, Bolivia; A restudy, *Am. Mineral.*, 1969, vol. 54, pp. 448–456.

Bertrand, E., Sur la molybdomenite (selenite de plomb), la cobaltomenite (selenite de cobalt) et 1'acide selenieux de Cacheuta (La Plata), *Bull. Soc. Mineral. France*, 1882, no 5, pp. 90–92.

Charykova M. V., Krivovichev V. G., Lelet M. I., Yakovenko, O.S., Suleimanov, E.V., Depmeier, W., Semenova, V.S., ans Zorina, M.I., A calorimetric and thermodynamic investigation of the synthetic analogues of cobaltomenite, $CoSeO_3 \cdot 2H_2O$, and ahlfeldite, $NiSeO_3 \cdot 2H_2O$, *Am. Mineral.*, 2014, vol. 99, pp. 742–748.

Charykova, M.V., Fokina, E.L., Klimova, E.V., Krivovichev, V.G., and Semenova, V.V., Thermodynamics of arsenates, selenites, and sulfates in the oxidation zone of sulfide ores. IX. Physicochemical formation conditions and thermal stability of zinc selenites, *Geol. Ore Deposits*, 2014, vol. 56, spec. issue 8 (Zapiski Russian Mineral. Soc.), pp. 546–552. (2013)

Charykova, M.V., Krivovichev, V.G., and Depmeir, W., Selenites and sulfates: System Ni^{2+}, Co^{2+} // SeO_3^{2-}, SO_4^{2-} – H_2O—thermodynamical analysis and geological applications, *Zapiski RMO* (*Proc. Russian Miner. Soc.*), 2007, spec. issue, pp. 247–267.

Charykova, M.V., Krivovichev, V.G., Yakovenko, O.S., Semenova, V.V., Semenov, K.N., and Depmeier, W., Thermodynamics of arsenates, selenites, and sulfates in the oxidation zone of sulfide ores: VI. Solubility of synthetic analogs of ahlfeldite and cobaltomenite at 25°C, *Geol. Ore Deposits*, 2012, vol. 55, spec. issue 8 (Zapiski Russian Mineral. Soc.), pp. 638–646.

Charykova, M.V., Krivovichev, V.G., Yakovenko, O.S., Semenova, V.V., Semenov, K.N., and Depmeier, W., Thermodynamics of arsenates, selenites, and sulfates in the oxidation zone of sulfide ores: Part VII. Solubility of synthetic analogs of erythrite and annabergite at 25°C, *Geol. Ore Deposits*, 2013, vol. 55, spec. issue 7 (Zapiski Russian Mineral. Soc.), pp. 525–531.

Engelen, B., Baumer, U., Hermann, B., Muller, H., and Unterderweide, K., Zur Polymorphie und Pseudo-symmetrie der Hydrate $MSeO_3 \cdot H_2O$ (M = Mn, Co, Ni, Zn, Cd), *Z. Anorg. Allg. Chem.*, 1996, vol. 622, pp. 1886–1892.

Fokina, E.L., Klimova, E.V., Charykova, M.V., Krivovichev, V.G., Platonova, N.V., Semenova, V.V., and Depmeier, W., The thermodynamics of arsenates, selenites, and sulfates in the oxidation zone of sulfide ores: VIII. Field of thermal stability of synthetic analog of chalcomenite, its dehydration and dissociation, *Geol. Ore Deposits*, 2014, vol. 56, spec. issue 7 (Zapiski Russian Mineralogical Society), pp. 538–545.

Herzenberg, R. and Ahlfeld, F., Blockit, ein neues Selenerz aus Bolivien, *Zentralbl. Mineral. Geol. Palaeontol. Abt. A.,* 1935, S. 277–279.

Larrañaga A., Mesa J. L., Pizarro J. L., Pena, A., Chapman, J.P., Arroortua, M.I., and Rojo, T., Thermal, spectroscopic and magnetic properties of the $Co_xNi_{1-x}(SeO_3) \cdot 2H_2O$ ($x = 0$, 0.4, 1) phases. Crystal structure of $Co_{0.4}Ni_{0.6}(SeO_3) \cdot 2H_2O$, *Mater. Res. Bul.*, 2005, vol. 40, pp. 781–793.

Makatun, V.N., Melnikova, R.Ya., and Barannikova, T.I. Structure of monohydrated selenites of transitional metals, *Strukt. Khim.*, 1975, vol. 1, pp. 920–925.

Makatun, V.N., Melnikova, R.Ya., and Pechkovsky, V.V. Lowest hydrates of cobalt selenites, *Izv. Akad. Sci. BSSR, Ser. Khim. Nauk,* 1974, no. 1, pp. 72–75.

Makatun, V.N., Melnikova, R.Ya., Pechkovsky, V.V. and Afanasiev, M.L., On dissociation of coordinated water in solid hydrates, *Dokl. AN SSSR*, 1973, vol. 213, pp. 353–355.

Martens, W.N., Kloprogge, J.T., Frost, R.L., and Rintoul, L. Site occupancy of Co and Ni in erythrite–annabergite solid solutions deduced by vibrational spectroscopy, *Can. Mineral.*, 2005, vol. 43, pp. 1065–1075.

Sturman, B.D. and Mandarino, J.A. The ahlfeldite–cobaltomenite series, *Can. Mineral.*, 1974, vol. 12, pp. 304–307.

Vlaev, L.T., Genieva, S.D., and Georgieva, V.G. Study of the crystallization fields of nickel(II) selenites in the system $NiSeO_3$–SeO_2–H_2O, *J. Therm. Anal. Calorim.*, 2006, vol. 86, pp. 449–456.

Vlaev, L.T., Genieva, S.D., and Gospodinov, G.G., Study of the crystallization fields of cobalt (II) selenites in the system $CoSeO_3$–SeO_2–H_2O, *J. Therm. Anal. Calorim.*, 2005, vol. 81, pp. 469–475.

Wildner, M., Crystal structure refinements of synthetic cobaltomenite ($CoSeO_3 \cdot 2H_2O$) and ahlfeldite ($NiSeO_3 \cdot 2H_2O$), *Neues Jahrb. Mineral. Monatsh.*, 1990, pp. 353–362.

Wildner, M., Crystal structures of $Co_3(SeO_3)_3 \cdot H_2O$ and $Ni_3(SeO_3)_3 \cdot H_2O$, two new isotypic compounds, *Monatsh. Chem.*, 1991, vol. 122, pp. 585–594.

Translated by I. Baksheev